Stereotactic radiotherapy plus whole-brain radiation therapy vs stereotactic radiosurgery alone for treatment of brain metastases: a randomized controlled trial. JAMA 2006;295: 2483-2491.

[17] Grimm SA. Treatment of brain metastases: chemotherapy. Curr Oncol Rep 2012;14(1): 85-90.

[18] Drappatz J, Wen PY. Chemotherapy and targeted molecular therapies for brain metastases. Expert Rev Neurother 2006;6(10): 1465-1479.

[19] van den Bent MJ. The role of chemotherapy in brain metastases. Eur J Cancer 2003;39(15): 2114-2120.

[20] Walbert T, Gilbert MR. The role of chemotherapy in the treatment of patients with brain metatstases from solid tumors. Int J Clin Oncol 2009;14(4): 299-306.

NEUROPATHOLOGY

Neuropathology 2013; **33**, 162–174 doi:10.1111/j.1440-1789.2012.01344.x

Original Article

Bimodal anti-glioma mechanisms of cilengitide demonstrated by novel invasive glioma models

Manabu Onishi,[1] Tomotsugu Ichikawa,[1] Kazuhiko Kurozumi,[1] Kentaro Fujii,[1] Koichi Yoshida,[1] Satoshi Inoue,[1] Hiroyuki Michiue,[1] E. Antonio Chiocca,[2] Balveen Kaur[3] and Isao Date[1]

[1]Department of Neurological Surgery, Okayama University Graduate School of Medicine, Dentistry and Pharmaceutical Sciences, Okayama, Japan, [2]Department of Neurosurgery, Brigham and Women's/Faulkner Hospital, Boston, Massachusetts, and [3]Dardinger Laboratory for Neuro-oncology and Neurosciences, Department of Neurological Surgery, The Ohio State University, Columbus, Ohio, USA

Integrins are expressed in tumor cells and tumor endothelial cells, and likely play important roles in glioma angiogenesis and invasion. We investigated the anti-glioma mechanisms of cilengitide (EMD121974), an αvβ3 integrin inhibitor, utilizing the novel invasive glioma models, J3T-1 and J3T-2. Immunohistochemical staining of cells in culture and brain tumors in rats revealed positive αvβ3 integrin expression in J3T-2 cells and tumor endothelial cells, but not in J3T-1 cells. Established J3T-1 and J3T-2 orthotopic gliomas in athymic rats were treated with cilengitide or solvent. J3T-1 gliomas showed perivascular tumor cluster formation and angiogenesis, while J3T-2 gliomas showed diffuse single-cell infiltration without obvious angiogenesis. Cilengitide treatment resulted in a significantly decreased diameter of the J3T-1 tumor vessel clusters and its core vessels when compared with controls, while an anti-invasive effect was shown in the J3T-2 glioma with a significant reduction of diffuse cell infiltration around the tumor center. The survival of cilengitide-treated mice harboring J3T-1 tumors was significantly longer than that of control animals (median survival: 57.5 days and 31.8 days, respectively, $P < 0.005$), while cilengitide had no effect on the survival of mice with J3T-2 tumors (median survival: 48.9 days and 48.5, $P = 0.69$). Our results indicate that cilengitide exerts a phenotypic anti-tumor effect by inhibiting angiogenesis and glioma cell invasion. These two mechanisms are clearly shown by the experimental treatment of two different animal invasive glioma models.

Correspondence: Tomotsugu Ichikawa, MD, PhD, Department of Neurological Surgery, Okayama University Graduate School of Medicine, Dentistry and Pharmaceutical Sciences, 2-5-1 Shikata-cho, Kita-ku, Okayama 700-8558, Japan. Email: tomoichi@cc.okayama-u.ac.jp
[Correction added on 28 September 2012, after first online publication: Author affiliations for E. Antonio Chiocca and Balveen Kaur were amended]

Received 20 June 2012; revised 7 August 2012 and accepted 9 August 2012; published online 19 September 2012.

Key words: angiogenesis, animal model, glioma, integrin, invasion.

INTRODUCTION

Gliomas are the most frequent primary intracranial neoplasm in adults and are invariably fatal. The median survival of aggressively treated patients with glioblastoma multiforme (GBM) is approximately 14.6 months.[1] The resistance of gliomas to the conventional therapeutic regimen of surgery, radiotherapy and chemotherapy has prompted many investigators to seek novel therapeutic approaches for this fatal disease.[2]

Two major aspects of glioma biology are the formation of new blood vessels through angiogenesis and the invasion of glioma cells via white matter tracts, which are the hallmarks of GBM.[3] The formation of abnormal tumor vasculature is one of the major reasons for the resistance of these tumors to treatment.[4] Inhibitors of angiogenesis can suppress tumor growth in preclinical models and have entered the clinic as prospective anticancer therapeutics.[5] Specifically, the administration of bevacizumab, a humanized monoclonal antibody against VEGF, in combination with irinotecan, a topoisomerase inhibitor, significantly improves outcome among recurrent patients.[6,7] However, de Groot *et al.*[8] showed that glioma cases developed an apparent phenotypic shift to a predominantly infiltrative pattern of tumor progression after treatment with bevacizumab. Thus, in addition to anti-angiogenesis therapy, successful treatment strategies for GBM may require the concomitant targeting of tumor cell invasion.[9]

Integrins are expressed in tumor cells and tumor endothelial cells,[10] and they play important roles in angiogenesis and invasion in gliomas.[11–13] αvβ3 and αvβ5 integrins regulate cell adhesion,[14,15] and inhibitors of these integrins suppress tumor growth in certain pre-clinical

models.[16] Therefore, integrins are being investigated as therapeutic targets in gliomas.

Cilengitide (EMD121974), a cyclic arginine-glycine-aspartic acid pentapeptide, is an αvβ3 integrin antagonist that induces anoikis in angiogenic blood vessels and brain tumor cells *in vitro*.[17,18] Cilengitide may inhibit tumor growth by at least two mechanisms: by targeting the tumor cells directly and by inhibiting tumor angiogenesis.[2,17,19] However, these mechanisms were not elucidated in invasive brain tumor models in animals.

We have established two new cell line-based animal models of invasive glioma, J3T-1 and J3T-2. These animal models histologically recapitulate two invasive and angiogenic phenotypes, namely angiogenesis-dependent and -independent invasion, which are also observed in human glioblastoma.[4,20] In short, J3T-1 cells form well demarcated and highly angiogenic tumors in rat brains, and clusters of tumor cells are seen around dilated, newly developed vessels in the adjacent normal brain. Therefore, J3T-1 gliomas express angiogenesis-dependent invasion and growth. In contrast, J3T-2 cells form poorly demarcated tumors, where the tumor cells gradually disperse from the tumor center to the normal brain parenchyma. Single cells also invade the normal brain parenchyma along white matter tracts. Therefore, J3T-2 gliomas express angiogenesis-independent invasion and growth.

To our knowledge, there are no published data demonstrating the anti-angiogenic or anti-invasive effects of cilengitide on gliomas using invasive animal models. Investigating the effects of cilengitide poses a challenge because most of the conventional animal models fail to mimic the invasiveness and angiogenesis of human glioma. Here, we investigated the antitumor effects of cilengitide on two experimental animal models of malignant glioma, J3T-1 and J3T-2.

MATERIALS AND METHODS

Glioma cell lines

Two cell lines, J3T-1 and J3T-2, were developed from the same parental J3T canine glioma cell line (a generous gift from Dr. Michael E. Berens; Translation Genomics Research Institute, Phoenix, AZ, USA), as previously described.[4,21] J3T-1 cells and J3T-2 cells were seeded on tissue culture dishes (BD Falcon, Franklin Lakes, NJ, USA) and cultured in Dulbecco's Modified Eagle's Medium (DMEM) supplemented with 10% fetal bovine serum (FBS), 100 units of penicillin and 0.1 mg/mL of streptomycin.

Cell surface immunofluorescence assay

J3T-1 and J3T-2 cells were seeded onto four-chamber polystyrene vessel tissue culture-treated glass slides (BD Falcon) and incubated overnight. For immunofluorescence, the cells were fixed in 4% paraformaldehyde in phosphate-buffered saline (PBS) for 15 min. After the cells were fixed, they were rinsed three times with PBS. Nonspecific binding was blocked by incubation in a blocking buffer containing 2% bovine serum albumin (BSA) in PBS for 30 min at room temperature. The cells were incubated overnight at 4°C with a mouse monoclonal anti-αvβ3 integrin antibody (Millipore Corporation, Billerica, MA, USA) diluted 1:100 in blocking buffer. The cells were washed three times in blocking buffer for 5 min before incubation with a secondary anti-mouse CY3-conjugated antibody (Jackson ImmunoResearch Laboratories, Inc., West Grove, PA, USA) diluted 1:300 in blocking buffer for 2 h at room temperature in the dark. After three washes in PBS, the cells were counterstained with 4′, 6-diamino-2-phenylindole (DAPI, 1:500; Invitrogen, Carlsbad, CA, USA) (100 ng/mL) for 20 min at room temperature. The slides were washed three times in PBS and mounted.

Tube formation assay

An angiogenesis assay kit (Kurabo, Osaka, Japan) was used according to the manufacturer's instructions. Briefly, human umbilical vein endothelial cells (HUVECs), co-cultured with neonatal normal human dermal fibroblasts (NHDFs),[22] were treated with various concentrations of cilengitide (0, 0.1, 0.5 or 1.0 or 2.0 μmol/L) and VEGF (10 ng/mL) added to the medium. Cilengitide was generously provided by Merck KGaA, Darmstadt, Germany and Cancer Therapy Evaluation Program (CTEP), the National Cancer Institute, NIH, Bethesda, MD, USA. Suramin (50 μmol/L) was used as a positive anti-angiogenic control. The medium was changed every 3 days. After 10 days, the dishes were washed with PBS and fixed with 70% ethanol at 4°C. After the fixed cells were rinsed three times with PBS, the cells were incubated with mouse anti-human CD31 antibody (Kurabo, Osaka, Japan) diluted 1:4000 in PBS containing 1% BSA for 60 min. After washing three times with 1% BSA-PBS, the cells were incubated with goat anti-mouse IgG-alkaline phosphatase conjugate. Metal-enhanced 3, 3′-diamino-benzidine-tetrahydrochloride (DAB) was used as the substrate with the reaction yielding a dark reddish-brown insoluble end-product. Finally, the cells were washed five times with PBS and viewed under a microscope (BZ-8000, Keyence, Osaka, Japan). The area and tube length were measured quantitatively with the Kurabo angiogenesis image analyzer in five different fields per well and statistically analyzed.[23]

Effects of cilengitide on cultured glioma cells

J3T-1 and J3T-2 cells were seeded on six-well plates (1.0×10^4 cells/well) and cultured in DMEM supplemented

with 10% FBS. Cilengitide (0, 0.1, 0.5 or 1.0 μmol/L) was added to the medium after 24 h of incubation. Each experiment was performed in triplicate. After incubation for 120 h at 37°C, the cells were examined for morphological changes. Non-adherent cells were removed by gentle washing twice with PBS, and the attached cells were then trypsinized and counted. The cell counts at 24 and 120 h incubation were compared and the cell proliferation rate was calculated.[17] Apoptotic cells were detected with the In Situ Cell Death Detection Kit (Roche, Basel, Switzerland) according to the manufacturer's instructions.

Invasive glioma xenograft models

All experimental animals were housed and handled in accordance with the guidelines of the Okayama University Animal Research Committee. Before implantation, 85–90% confluent J3T-1 and J3T-2 cells were trypsinized, rinsed with DMEM supplemented with 10% FBS, and centrifuged at 100 × g for 5 min. The resulting pellet was then resuspended in PBS, and the cell concentration was adjusted to 1.0×10^5 cells/μL. For each cell line, athymic rats (F344/N-nu/nu; CLEA Japan, Inc., Tokyo, Japan) were injected with 5 μL J3T-1 or J3T-2 cells and athymic mice (balb/c-nu/nu; CLEA Japan, Inc, Tokyo, Japan) were injected with 2 μL J3T-1 or J3T-2 cells. The animals were anesthetized and placed in stereotactic frames (Narishige, Tokyo, Japan) with their skulls exposed. Tumor cells were injected with a Hamilton syringe (Hamilton, Reno, NV, USA) into the right frontal lobe (in the athymic rats: 4 mm lateral and 1 mm posterior to the bregma at a depth of 4 mm; in the athymic mice: 3 mm lateral and 1 mm anterior to the bregma at a depth of 3 mm), and the syringe was slowly withdrawn after 5 min to prevent reflux. The skulls were then cleaned, the holes were sealed with bone wax, and the incision was sutured.

Cilengitide or PBS was administered three times/week intraperitoneally (for the athymic mice: 200 μg/100 μL PBS; for the athymic rats: 1000 μg/500 μL PBS) starting on day 5 after tumor cell implantation. To analyze survival time, the J3T-1 and J3T-2 athymic mice xenograft models were monitored.

Histopathological analysis of glioma in rats

For histopathological analysis, athymic rats harboring J3T-1 or J3T-2 brain tumors were sacrificed at 35 days after tumor implantation. Before immunohistochemistry and HE staining, athymic rats were anesthetized, euthanized by cardiac puncture, perfused with 100 mL PBS, and fixed with 200 mL 4% paraformaldehyde. The brains were removed and stored in 4% paraformaldehyde for at least 24 h.

For HE staining, the sections were immersed in hematoxylin for 1 min and rinsed with tap water. The sections were then immersed in an eosin stain for 1–2 min and rinsed with tap water.

For immunohistochemical staining of αvβ3 integrin, after deparaffinization in xylene and rehydration in decreasing concentrations of ethanol, 4-μm thick sections were incubated in 0.3% H_2O_2 (30 min) and autoclaved for 10 min at 121°C in distilled water. After washing three times in PBS, the sections were incubated at room temperature for 1 h with a mouse monoclonal anti-αvβ3 integrin antibody (Millipore) diluted 1:100 in a solution of PBS and 5% skimmed milk. The Dako Cytomation Envision+ System-HRP Kit was then applied according to the manufacturer's protocol (DakoCytomation, Carpentaria, CA, USA). After three washes in PBS, the sections were counterstained with hematoxylin.

For immunofluorescent staining, snap-frozen tissue samples were embedded in a compound of optimal cutting temperature for cryosectioning, and 16-μm cryostat sections were processed for indirect immunofluorescence. The slides were incubated with 10% horse serum in PBS at room temperature for 60 min, then overnight at 4°C with an anti-RECA (rat endothelial cell antigen)-1 antibody (Abcam, Cambridge, MA, USA) diluted 1:20 in 1% horse serum in PBS. After three washes with PBS for 5 min, the slides were incubated with a Cy3-conjugated anti-mouse antibody (Jackson ImmunoResearch Laboratories) and DAPI (1:500) (Invitrogen) in PBS for 60 min. The slides were then washed in PBS and mounted.

Statistical analysis

Student's *t*-test was used to test for statistical significance. Data were presented as the means ± standard error. Kaplan–Meier curves were compared using the log-rank test. Statistical analysis was performed using Stat View statistical software (version 5.0; SAS Institute Inc., Cary, NC, USA).

RESULTS

Immunohistochemical analysis of αvβ3 integrin expression in the two glioma cell lines

Immunofluorescence assays were conducted to determine the expression of αvβ3 integrin in J3T-1 and J3T-2 cells. Cultured J3T-1 cells were not immunopositive for αvβ3 integrin (Fig. 1A). In contrast, robust expression of αvβ3 integrin was observed on the surface of J3T-2 cells (Fig. 1B).

Immunohistochemical staining for αvβ3 integrin was also performed in brain slices of animals harboring either J3T-1 or J3T-2 brain tumors. The J3T-1 glioma cells that were clustered around the dilated tumor vessels were

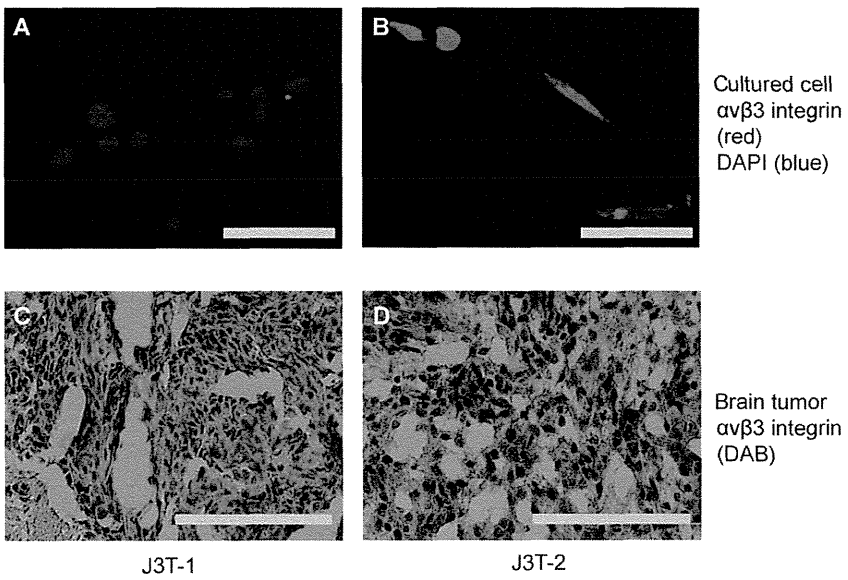

Fig. 1 *In vitro* and *in vivo* immunohistochemical analysis of αvβ3 integrin expression in J3T-1 and J3T-2 cells. Immunofluorescence of αvβ3 integrin in cultured cells was negative in J3T-1 cells (A) and positive on the surface of J3T-2 cells (B). Scale bar = 50 μm. Immunohistochemical staining for αvβ3 integrin in brain slices revealed that the J3T-1 glioma cells were negative for αvβ3 integrin, yet the endothelial cells of dilated tumor vessels were positive (C). J3T-2 glioma cells were diffusely positive for αvβ3 integrin (D). Scale bar = 50 μm.

negative for αvβ3 integrin, yet the endothelial cells of dilated tumor vessels were clearly positive for αvβ3 integrin (Fig. 1C). J3T-2 glioma cells were diffusely positive for αvβ3 integrin. There were no dilated vessels in the J3T-2 tumors that were positive for αvβ3 integrin (Fig. 1D).

Effects of cilengitide on endothelial cells *in vitro*

To investigate the effects of cilengitide on endothelial cells, a tube formation assay using HUVECs co-cultured with NHDFs was performed. HUVECs formed tubes in the medium containing VEGF (Fig. 2A). The addition of cilengitide (0.1 μmol/L, 0.5 μmol/L, 1.0 μmol/L) to the culture medium inhibited tube formation in a concentration-dependent manner (Fig. 2B–D). All HUVECs and NHDFs detached from the dishes when the concentration of cilengitide was 2.0 μmol/L. An anti-VEGF drug (suramin: 50 μmol/L) also inhibited tube formation (Fig. 2E). The average tube length under each condition was computed (0 μmol/L cilengitide: $1.45 \times 10^4 \pm 4.9 \times 10^2$ pixels; 0.1 μmol/L cilengitide: $1.24 \times 10^4 \pm 5.8 \times 10^2$ pixels; 0.5 μmol/L cilengitide: $1.04 \times 10^4 \pm 5.8 \times 10^2$ pixels; 1.0 μmol/L cilengitide: $0.90 \times 10^4 \pm 4.8 \times 10^2$ pixels ($P < 0.05$); 50 μmol/L suramin: $0.99 \times 10^4 \pm 6.8 \times 10^2$ pixels) (Fig. 2F). Quantitative analysis of tube length confirmed that cilengitide inhibited angiogenesis *in vitro* in a concentration-dependent manner.

Cytotoxic effects of cilengitide on the two invasive glioma cell lines *in vitro*

The direct effects of cilengitide were investigated on glioma cells *in vitro*. J3T-1 and J3T-2 cells were incubated with cilengitide at concentrations of 0–1.0 μmol/L. Treated cells were examined for morphologic changes after 120 h. Originally, J3T-1 cells in culture were composed of bipolar cells and spherical cells. When the cells were incubated with cilengitide, the number of spherical cells increased in a dose-dependent manner (Fig. 3A). However, there was no significant increase in the number of detached cells. Before administration of cilengitide, J3T-2 cells were mostly composed of bipolar cells. They became spherical and agglutinated when cilengitide was added to the incubation media. Some of these deformed cells detached from the plate (Fig. 3A). The detached J3T-2 cells were not viable, as indicated by unsuccessful attempts of re-plating in media containing no cilengitide. To confirm the apoptosis of deformed glioma cells treated with cilengitide, cells were stained with the In Situ Cell Death Detection Kit containing tetramethylrhodamine (TMR) red. J3T-1 cells were negative for apoptosis, while J3T-2 cell clusters were positive (Fig. 3B).

The attached cell count was measured and compared between 24 and 120 h after incubation (Fig. 3C). The counts of J3T-1 cells did not change with any concentrations of cilengitide (0–1.0 μmol/L), whereas the counts of J3T-2 cells decreased in a dose-dependent manner. The count of J3T-1 cells incubated with or without cilengitide (1.0 μmol/L) increased by 19.2-fold and 18.9-fold, respectively. The count of J3T-2 cells incubated with or without cilengitide increased by 13.2-fold and 19.6-fold, respectively. Therefore, cilengitide significantly inhibited the proliferation of J3T-2 cells ($P < 0.05$), but not J3T-1 cells ($P = 0.992$).

Anti-angiogenic effects of cilengitide in J3T-1 gliomas in rats

Angiogenic activity was histopathologically evaluated using the J3T-1 angiogenesis-dependent invasive glioma

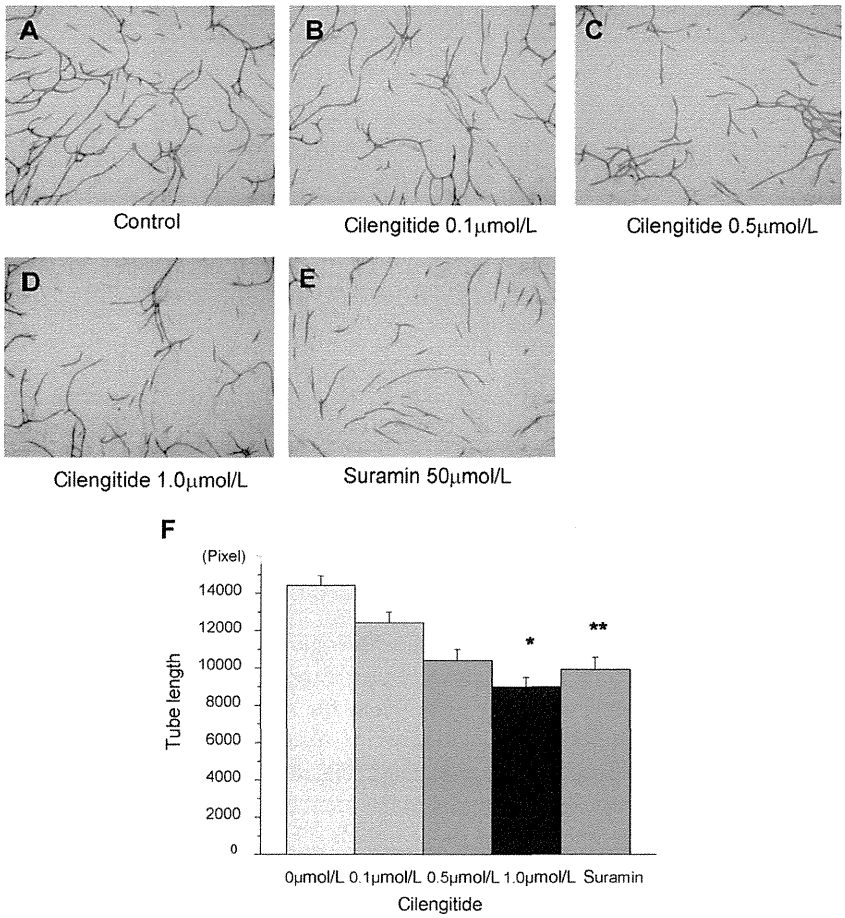

Fig. 2 Effects of cilengitide on tube formation. Human umbilical vein endothelial cells (HUVECs) co-cultured with fibroblasts and VEGF (10 ng/mL) without cilengitide (A) or with cilengitide (0.1, 0.5, 1.0 μmol/L) (B–D) or suramin (50 μmol/L) (E) for 10 days. The length of tube-like structures was measured quantitatively using an image analyzer. The tube length was significantly shortened with cilengitide treatment in a concentration-dependent manner (*$P = 0.0062$, **$P = 0.0089$) (mean ± SE, $n = 6$).

models in rats. Low magnification of HE staining of J3T-1 control tumors revealed that J3T-1 cells formed clusters in the adjacent normal brain (Fig. 4A). Immunofluorescence staining (vascular endothelial cells: RECA-1, red; nuclei: DAPI, blue) of J3T-1 control tumors clearly showed this tumor's angiogenesis-dependent invasive phenotype as described in a former study.[20] In short, J3T-1 cells were clustered, with these clusters centered on dilated neovascular vessels, and invaded along the perivascular area (Fig. 4C). When animals were treated with intraperitoneal cilengitide ($n = 3$), brain tumors showed an angiogenesis-dependent pattern (Fig. 4B). There was no significant difference in the invasive pattern between cilengitide-treated and control tumors. However, the extent of spread of invasion clusters was significantly decreased in animals treated with cilengitide compared with the control animals. Furthermore, the diameter of the tumor clusters and its core vessels in the treated animals was smaller than that in the untreated animals (Fig. 4D).

To quantify the effect of cilengitide, the diameter of the tumor clusters around the neovasculature and the diameter of the tumor vessels were measured with ImageJ software (http://rsb.info.nih.gov/ij). The diameter of tumor clusters in control and cilengitide-treated animals was 111 ± 6.4 μm and 86.3 ± 6.8 μm, respectively ($P < 0.005$) (Fig. 4E). The diameter of core vessels in control and treated animals was 16.3 ± 1.0 μm and 12.5 × ± 1.0 μm, respectively ($P < 0.005$) (Fig. 4F).

Anti-invasive effects of cilengitide demonstrated in J3T-2 gliomas in rats

The effect of cilengitide on the diffuse invasive activity of glioma cells was histopathologically evaluated using J3T-2 angiogenesis-independent invasive glioma models in rats. Macroscopic examinations of HE staining of J3T-2 control tumors revealed that J3T-2 tumors strongly invaded the adjacent normal brain (Fig. 5A). Briefly, tumor cells gradually dispersed from the tumor center to the normal brain parenchyma with a cell density gradient, which meant that J3T-2 cells formed poorly demarcated tumors. Minimal angiogenesis was seen with only a small number of slightly dilated vessels at the tumor center. A similar invasive pattern was observed in animals treated with cilengitide ($n = 3$) (Fig. 5B). The merged immunofluorescence staining images (vascular endothelial cells: RECA-1, red; nuclei: DAPI, blue) revealed the tumor borders in more detail

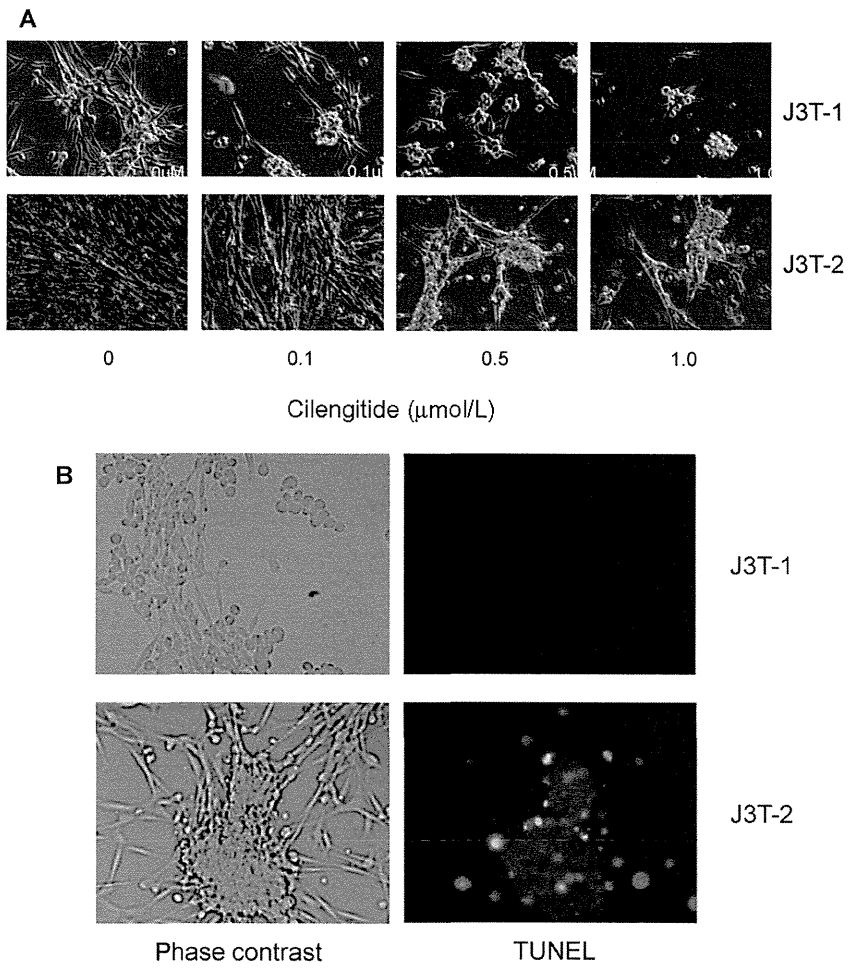

Fig. 3 Direct cytotoxic effects of cilengitide on J3T-1 and J3T-2 glioma cells in culture. Morphological changes were observed after cilengitide treatment (0.1, 0.5 or 1.0 μmol/L) in a dose-dependent manner. Some of the J3T-1 cells became spherical but did not detach from the plate (upper panel in A). J3T-2 cells become spherical and agglutinated. Some of the deformed cells detached from the plate (lower panel in A). Deformed cells were stained red by TUNEL treatment in J3T-2 cells (lower panel in B), but not in J3T-1 cells (upper panel in B). A significant inhibitory effect on the proliferation of J3T-2 cells was observed ($*P < 0.005$), but was not seen in J3T-1 cells ($P = 0.992$) (C) (mean ± SE, $n = 6$). —●—, J3T-1; —▲—, J3T-2.

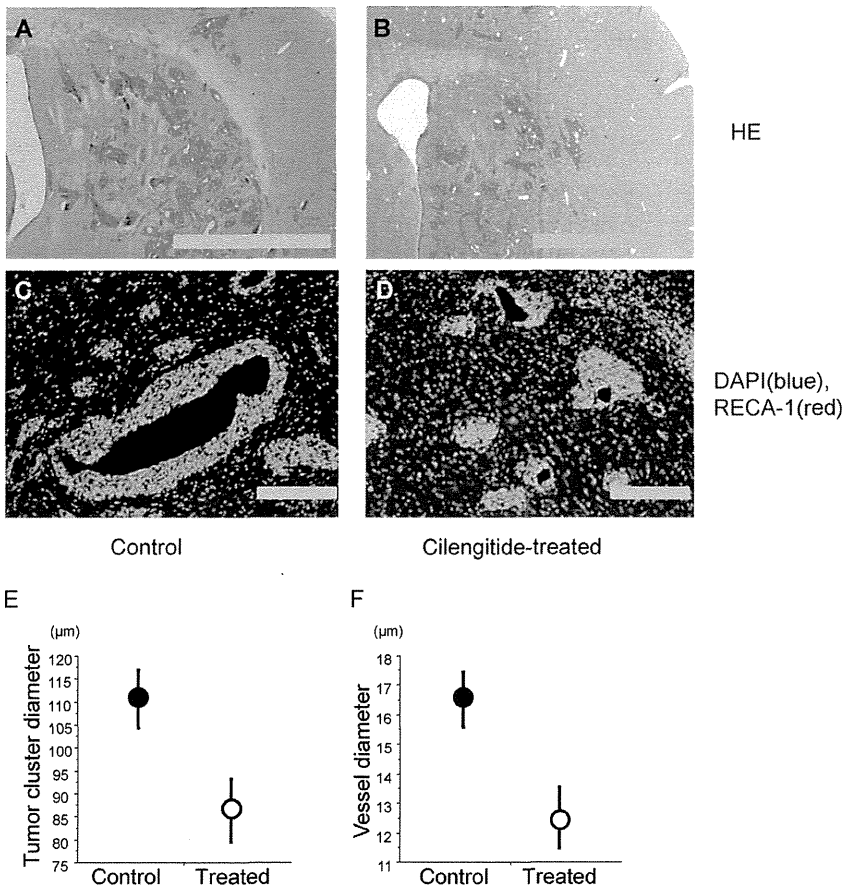

Fig. 4 Anti-angiogenic effects of cilengitide on J3T-1 gliomas in rats. Low magnification of HE staining of control tumors (A) and cilengitide-treated tumors (B) revealed the same invasive pattern of cluster formation around dilated neovasculature. However, the spread of the invasion clusters was significantly smaller in animals treated with cilengitide compared with control animals. Scale bar = 2.0 mm. When examined with immunofluorescence staining (vascular: RECA-1 (rat endothelial cell antigen-1), red; nuclei: DAPI (4′, 6-diamino-2-phenylindole), blue), the diameter of the tumor clusters and its core vessels in cilengitide-treated animals (D) were smaller than that in untreated animals (C). Scale bar = 100 μm. The quantitative analysis of the diameter of the tumor clusters (E) and its core vessels (F) revealed a significant decrease in cilengitide-treated animals compared with control animals ($P < 0.005$) (mean ± SE, $n = 3$).

(Fig. 5C,D). The distribution area of diffuse tumor cell infiltration around the tumor center was smaller in cilengitide-treated animals compared with control animals. To quantify the cell density, the merged images from the J3T-2 tumor center to the normal subcortex, avoiding the corpus callosum, were partitioned into 22 equal areas (200 μm×100 μm), and the nuclei (DAPI, blue) in each area were counted ($n = 3$). The cell density at the tumor center was significantly higher in treated animals than in control animals (Fig. 5E). The cell density of control tumors was gradually reduced from the tumor center toward the normal brain parenchyma, while the cell density of treated tumors dropped steeply at the tumor border. There were no significant differences in cell numbers in the designated areas (200 μm×2200 μm) (control tumors: 1400 ± 31 cells; treated tumors: 1310 ± 72 cells; $P = 0.27$) (Fig. 5F).

The cytotoxic effects of cilengitide on J3T-1 and J3T-2 gliomas in rats

The cytotoxic effects of cilengitide on glioma cells *in vivo* were investigated using both rat brain tumor models. A subpopulation of apoptotic cells were visualized by TUNEL treatment using the In Situ Cell Death Detection Kit (apoptotic cells: TMR red; nuclei: DAPI, blue). The J3T-1 control tumor (Fig. 6A), J3T-1 cilengitide-treated tumor (Fig. 6B), J3T-2 control tumor (Fig. 6C), and J3T-2 cilengitide-treated tumor (Fig. 6D) sections from rat brains were prepared and assayed. These figures show a low number (2–3%) of apoptotic cells. To quantify the cytotoxic effect of cilengitide, the number of apoptotic cells per high-power field (HPF) in J3T-1 tumors (Fig. 6E) and J3T-2 tumors (Fig. 6F) were assessed. (J3T-1 control tumors: 5.75 ± 1.6 cells/HPF, J3T-1 cilengitide-treated tumors: 3.71 ± 0.6 cells/HPF, J3T-2 control tumors: 4.50 ± 1.1 cells/HPF, J3T-2 cilengitide-treated tumors: 5.83 ± 1.1 cells/HPF). There was no significant difference in apoptotic cells in the cilengitide-treated tumors compared with control tumors (J3T-1, $P = 0.5972$; J3T-2, $P = 0.4233$).

Survival analysis by using two different invasive glioma models

To evaluate the *in vivo* anti-tumor effect of cilengitide, the long-term survival of mice harboring J3T-1 or J3T-2 brain tumors was analyzed. Athymic mice harboring J3T-1 or J3T-2 brain tumors (12 animals each) were each divided

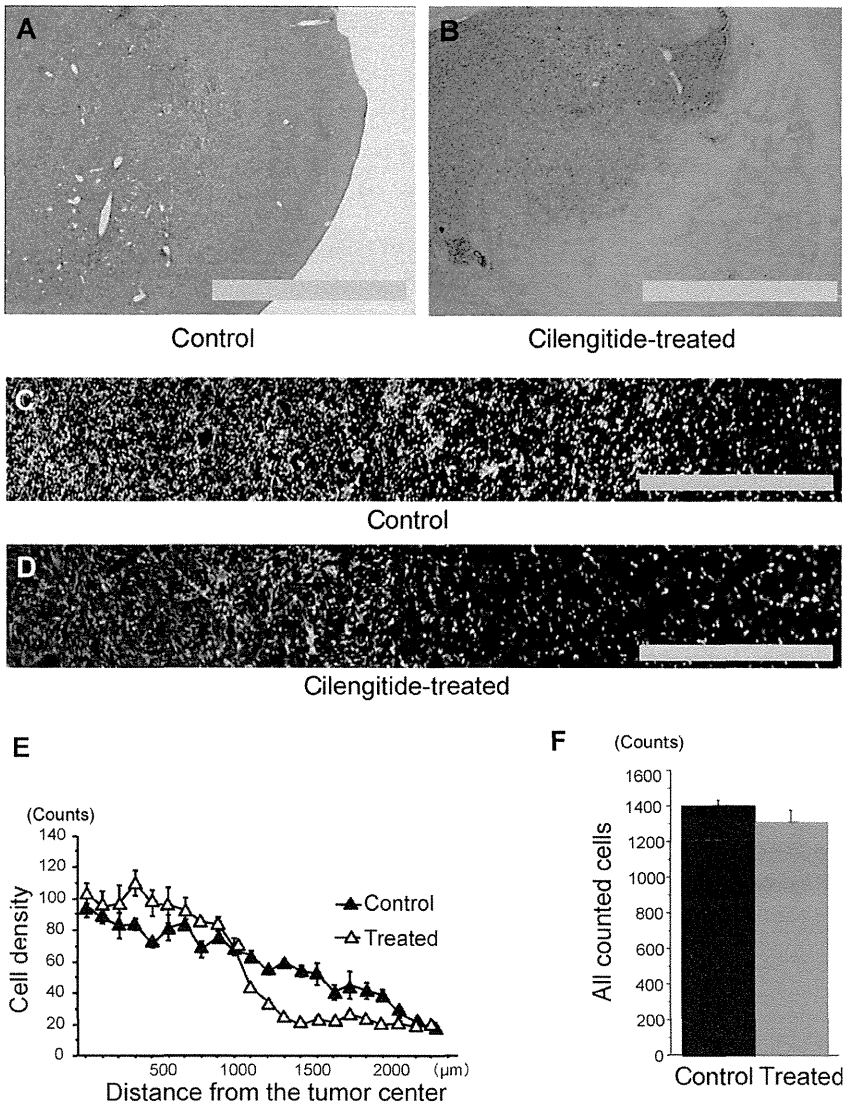

Fig. 5 Anti-invasive effects of cilengitide on J3T-2 gliomas in rats. HE staining of control tumors (A) and cilengitide-treated tumors (B) revealed that tumor cells gradually dispersed from the tumor center to the normal brain parenchyma with a cell density gradient in both tumors. Scale bar = 2 mm. Immunofluorescence staining (vascular: RECA-1 (rat endothelial cell antigen-1), red; nuclei: DAPI (4′, 6-diamino-2-phenylindole), blue) of control tumors (C) and cilengitide-treated tumors (D) revealed that the tumor borders of the treated tumors were more evident. Scale bar = 500 μm. The cell density was higher at the center of the tumor and lower at the periphery of the infiltration area in animals treated with cilengitide compared with control animals (E). There were no significant differences in the cell numbers in the examined areas (F) ($P = 0.27$) (mean ± SE, $n = 3$).

into two groups. The animals received either intraperitoneal cilengitide (200 μg/100 μL, three times/week) or PBS. The median survival was 57.5 days in animals bearing J3T-1 tumors treated with cilengitide, and 31.8 days in animals given PBS (Fig. 7A). A significant prolongation of survival by cilengitide administration was observed in animals harboring J3T-1 tumors ($P < 0.005$). In contrast, the survival of mice bearing J3T-2 gliomas was not prolonged by intraperitoneal cilengitide injection ($P = 0.69$) (Fig. 7B). The median survival of the animals with J3T-2 tumors treated either with cilengitide or PBS was 48.9 days or 48.5 days, respectively.

DISCUSSION

In the present study, we tested cilengitide on two invasive glioma animal models, J3T-1 (αvβ3 integrin-negative, angiogenesis-dependent invasive phenotype) and J3T-2 (αvβ3 integrin-positive, angiogenesis-independent invasive phenotype). *In vitro* proliferation of αvβ3 integrin-positive J3T-2 cells was significantly inhibited by cilengitide, whereas cilengitide treatment did not inhibit proliferation in αvβ3 integrin-negative J3T-1 cells. On the other hand, the survival of mice harboring J3T-1 tumors treated with cilengitide was significantly longer than control animals. Although the survival of mice harboring J3T-2 tumors treated with cilengitide was not prolonged, pathologic examination revealed that angiogenesis-independent, single-cell infiltration was clearly inhibited by cilengitide. These results mean that cilengitide has multi-modal anti-glioma mechanisms. This is the first study to show the bimodal mechanisms of the anti-tumor effect of cilengitide on glioma by using two animal invasive brain tumor models.

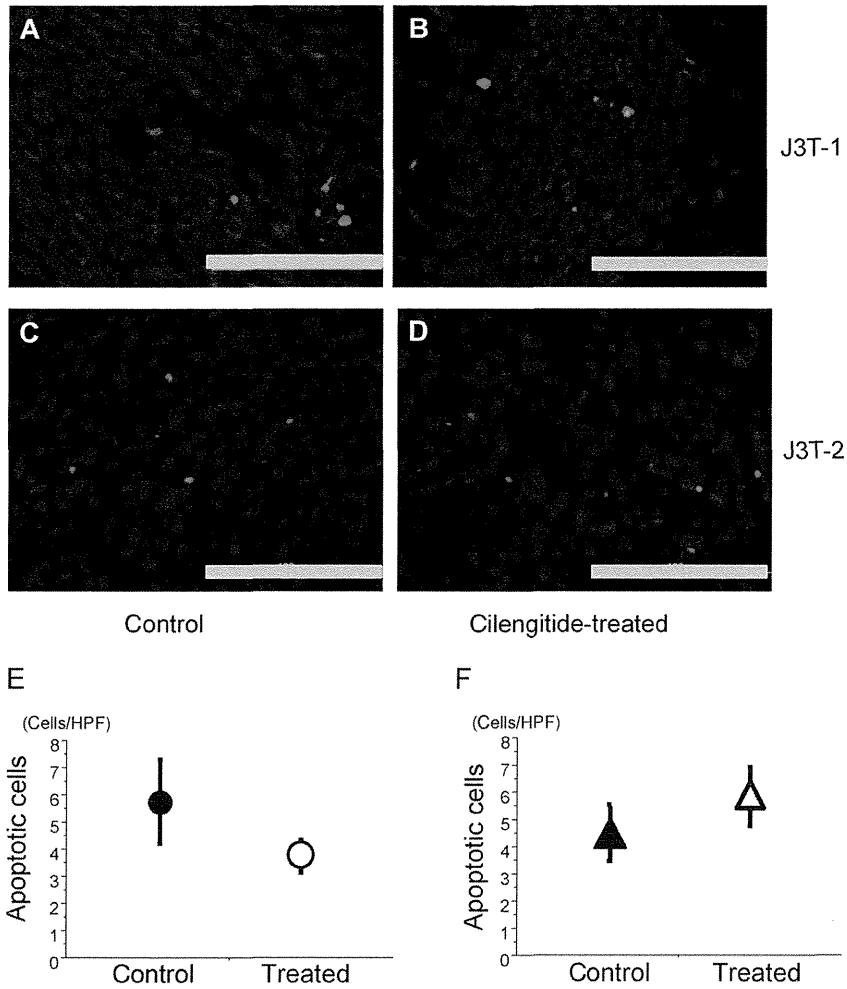

Fig. 6 Cytotoxic effects of cilengitide on J3T-1 and J3T-2 rat brain tumors. A subpopulation of apoptotic cells were visualized by TUNEL staining (apoptotic cells: tetramethylrhodamine (TMR) red; nuclei: DAPI (4′, 6-diamino-2-phenylindole), blue) of J3T-1 control tumors (A), J3T-1 cilengitide-treated tumors (B), J3T-2 control tumors (C), and J3T-2 cilengitide-treated tumors (D). Scale bar = 100 μm. The quantitative analysis of the number of the apoptotic cells/high power field (HPF) in J3T-1 tumors (E) and J3T-2 tumors (F) revealed no significant difference between control and cilengitide-treated animals (J3T-1, $P = 0.5972$; J3T-2, $P = 0.4233$) (mean ± SE, $n = 6$).

Cilengitide inhibited the adhesion and proliferation of αvβ3 integrin-positive J3T-2 cells in culture. Apoptosis of J3T-2 cells was also induced due to the loss of adherence to the plate, which is termed anoikis.[24] Cilengitide induces anoikis in brain tumor cells by inhibiting the phosphorylation of FAK, Src and Akt.[17,18] However, the results from our *in vivo* experiments did not show the cytotoxic effect of cilengitide on J3T-2 cells. As shown by pathological examination of animal brain tumors treated with cilengitide, apoptotic cell numbers did not increase in the integrin-positive J3T-2 brain tumor model. Furthermore, the survival of animals harboring J3T-2 gliomas was not prolonged by cilengitide. To our knowledge, there is no published data which shows cilengitide-induced anoikis in animal brain tumor models. This discrepancy between *in vitro* and *in vivo* results might be partly due to the difference in the dependency of adhesion molecules and the microenvironment. Many adhesion molecules other than αvβ3 integrin, such as cadherins and L1, might be involved in cell-cell or cell- extracellular matrix (ECM) adhesion *in situ* compared with the *in vitro* environment.[25,26] Therefore, blockade of only αvβ3 integrin cannot induce complete detachment of cells from surrounding tissues and subsequent anoikis.

Angiogenesis is the formation of new blood vessels by the rerouting or remodeling of existing ones, and is the primary method of vessel formation in gliomas. In this study, the efficient inhibition of angiogenesis was shown by the tube formation assay of HUVECs *in vitro*. Furthermore, prolonged survival after cilengitide administration was shown in animals harboring J3T-1 brain tumors, an angiogenesis-dependent invasive glioma model, but not in J3T-2 tumors, an angiogenesis-independent invasive glioma model. Yamada *et al.* reported that cilengitide is highly effective in suppressing blood vessel growth, thereby inhibiting the orthotopic growth of human GBM cells in animals.[27] Angiogenesis requires three distinct steps: (i) blood vessel breakdown; (ii) degradation of the vessel basement membrane and the surrounding ECM; and (iii) migration of endothelial cells and the formation of new blood vessels.[3] During the third step, endothelial cells proliferate and begin to migrate toward tumor cells

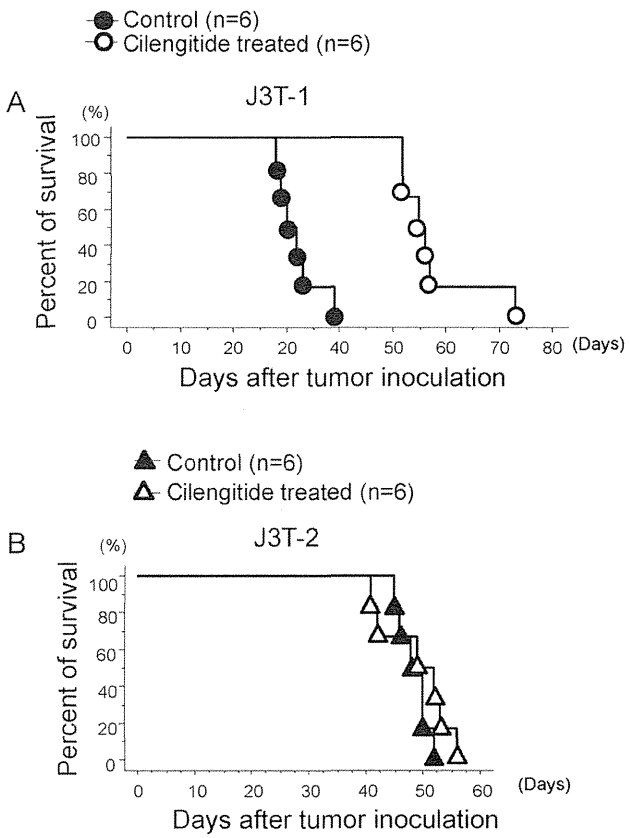

Fig. 7 Survival of athymic mice harboring J3T-1 or J3T-2 brain tumors treated with cilengitide. Kaplan–Meier survival analysis of athymic mice harboring intracranial J3T-1 (A) and J3T-2 (B) brain tumors treated with cilengitide or PBS. The survival time of J3T-1 glioma mice was significantly prolonged by the intraperitoneal injection of cilengitide (A) ($P < 0.005$) while the survival of J3T-2 glioma mice was not prolonged (B) ($P = 0.6889$). —●—▲—, control ($n = 6$); —○— —△—, cilengitide-treated ($n = 6$).

expressing pro-angiogenic compounds. Endothelial cell activation up-regulates the expression of cell surface adhesion/migration molecules, especially αvβ3 integrin, which results in an enhancement of endothelial cell adhesion and migration.[12,13] Cilengitide might prevent the third step of angiogenesis and reduce the size of tumor vessels. Thus, the anti-angiogenic effects of cilengitide are likely to be the main mechanism inhibiting angiogenic J3T-1 tumor growth.

Previously it was reported that there is a shift from the angiogenic to the invasive phenotype after anti-angiogenic therapy with use of an anti-VEGF antibody.[28–31] Invasion is another target for glioma therapy and glioma cell invasion requires four distinct steps: (i) detachment of invading cells from the primary tumor mass; (ii) adhesion to the ECM; (iii) degradation of the ECM; and (iv) cell motility and contractility.[3] During the second step, integrins allow glioma cells to adhere to the ECM. αvβ3 integrin, which binds to fibronectin, vitronectin and tenascin-C in the ECM, plays a central role in glioma invasion.[15] Platten *et al.* reported that inhibition of αvβ3 integrin decreased glioma cell motility *in vitro*.[32] Cilengitide might inhibit this second step, thereby suppressing the invasiveness of the glioma. This is the first study to show that cilengitide suppresses the angiogenesis-independent, single-cell infiltration of glioma cells in the animal J3T-2 brain tumor model. However, cilengitide had no survival benefit on J3T-2 brain tumors. This was because cilengitide had little direct cytotoxic effect on tumor cells *in situ*.

In the invading front of the glioma, most of the arteries have an intact blood–brain barrier (BBB) because single cell invasion is angiogenesis-independent.[20] Therefore, drugs must pass through the normal BBB to exert anti-invasive effects on invading cells. According to our results treating J3T-2 brain tumors with cilengitide, the drug apparently passes through the normal BBB. In a North American Brain Tumor Consortium (NABTC) study, increased intra-tumoral cilengitide levels were shown in patients with glioblastoma when cilengitide was administered 24 h before surgical debulking. This study confirms that cilengitide is effectively delivered into primary human GBM tumors.[33]

To analyze the mechanisms of angiogenesis and invasion of gliomas, and anti-glioma effects of drugs which target them, animal models which show angiogenic tumor growth or diffuse invasive growth are required. However, most of the conventional animal models show angiogenic tumor growth but fail to mimic the diffuse invasiveness of human glioma.[3] Therefore, analysis of the invasive ability of glioma has depended on *in vitro* evaluation systems. We have established two novel invasive animal glioma models, J3T-1 and J3T-2, from the same parental cells that separately reflect these two invasive phenotypes of human malignant gliomas.[4,20] J3T-1 gliomas demonstrate angiogenesis-dependent invasive growth that is limited to the perivascular space of newly developed blood vessels. On the other hand, J3T-2 gliomas showed angiogenesis-independent, diffusely invasive growth. The expression levels of integrins are also different between these models; J3T-1 is αvβ3 integrin-negative, while J3T-2 is αvβ3 integrin-positive.

These models were used to investigate separately the anti-angiogenic and anti-invasion effects of cilengitide. The most notable characteristics of our models, which make them ideal for studying cilengitide, are as follows. First, J3T-1 and J3T-2 brain tumor models histologically recapitulate both the invasive and angiogenic phenotypes observed in human glioma. Human gliomas consist of mixtures of these phenotypic subclones.[20] To clarify the anti-glioma mechanisms, models that exhibit each phenotype separately are needed. Second, J3T-1 and J3T-2 brain

tumor models are easily reproducible. Third, they consist of subclones established from the same parental cell. Thus, they should have similar genetic backgrounds (T Maruo, T Ichikawa, H Kanzaki, S Inoue, K Kurozumi, M Onishi, K Yoshida, H Kambara, M Ouchida, K Shimizu, S Tamaru, EA Chiocca, I Date, "Proteomics-based analysis of invasion-related proteins in malignant gliomas", submitted).

In this study, the anti-invasive effect of cilengitide was shown in animal brain tumor models. Also, the lack of a direct cytotoxic effect of cilengitide was demonstrated in animal models. Yamada *et al.* tested cilengitide in a U87 brain tumor model in mice.[27] Since U87 cells show well-demarcated, angiogenic and non-invasive growth *in vivo*, Yamada and colleagues could only examine the anti-angiogenic effect of cilengitide, but could not test an anti-invasive effect or a cytotoxic effect. Therefore, an *in vivo* evaluation system such as our paired invasive glioma models is necessary for the evaluation of novel therapeutic agents.

The formation of abnormal tumor vasculature and single-cell invasion into normal brain parenchyma are major reasons for the resistance of malignant glioma to conventional treatments. Our results showed that cilengitide exerts a bimodal anti-glioma effect with anti-angiogenic and anti-invasive effects. Therefore, cilengitide holds promise as a glioma therapy in the clinical setting.

There have been several reports that showed preliminary results of phase I or II studies of cilengitide for recurrent or newly diagnosed malignant glioma. Cilengitide monotherapy or combination treatment with radiation and/or temozolomide is well tolerated and exhibits modest anti-tumor activity.[34]

Bevacizumab, another anti-angiogenic agent, is a humanized monoclonal antibody against VEGF that demonstrates a strong anti-angiogenic effect in gliomas. However, bevacizumab induces a phenotypic shift in the glioma from angiogenic to diffusely invasive tumors leading to therapy-resistant tumor progression.[28–31] According to results from a limited number of studies, such phenotypic shift is not reported after cilengitide treatment. This might be partly because of cilengitide's bimodal anti-angiogenic and anti-invasive effects.

According to our results, cilengitide has a strong anti-tumor effect which is mainly dependent on the anti-angiogenic and anti-invasive effects but has little, if any, direct cytotoxic effect on glioma cells. Therefore, combination therapy with cytotoxic therapeutics, for example, radiation therapy, other chemotherapy or oncolytic virus therapy, would be effective. Alghisi *et al.* demonstrated that cilengitide elicits signaling events that disrupt vascular endothelial (VE)-cadherin localization at cellular contacts and increases the permeability of the endothelial monolayer. Therefore, the effects of cilengitide on endothelial cells make it a potentially well-suited drug to be combined with chemotherapeutic agents to improve drug delivery.[18] Several preclinical studies have shown an enhanced anti-tumor effect of cilengitide when administered in combination therapeutic regimens.[9,35–37] The anti-angiogenic effect of cilengitide also may enhance combined treatments. Mikkelsen *et al.* showed cilengitide did not influence the effect of radiation on U251 glioma cells but strongly amplified effects on endothelial cell survival *in vitro*. They also showed cilengitide treatment dramatically amplified the efficacy of radiation therapy in an animal glioma model.[38] Kurozumi and colleagues demonstrated the enhanced therapeutic efficacy of an oncolytic virus on experimental glioma with cilengitide pretreatment.[39] They showed oncolytic virus therapy-induced changes in the tumor microenvironment, such as increased tumor vascular permeability, leukocyte infiltration, and inflammatory cytokines, were inhibited by pretreatment with a single dose of cilengitide.

CONCLUSIONS

In conclusion, our results indicate that cilengitide exerts a phenotypic anti-tumor effect by inhibiting tumor angiogenesis and tumor cell invasion. These two mechanisms are clearly shown by the experimental treatment of two different animal invasive glioma models.

ACKNOWLEDGMENTS

This study was supported by grants-in-aid for Scientific Research from the Japanese Ministry of Education, Culture, Sports, Science, and Technology to T.I. (No. 19591675; no. 22591611), and K.K. (No. 20890133; no. 21791364). Cilengitide was generously provided by Merck Serono and the National Cancer Institute, NIH. We thank H. Wakimoto, M. Arao and A. Ishikawa for their technical assistance. The following medical students also contributed to the animal experiments: T. Mifune, S. Murai, M. Matsueda, H. Matsumoto and Y. Yoshida. Merck Serono has reviewed this publication; the views and opinions described in this publication do not necessarily reflect those of Merck Serono.

REFERENCES

1. Stupp R, Mason WP, van den Bent MJ *et al.* Radiotherapy plus concomitant and adjuvant temozolomide for glioblastoma. *N Engl J Med* 2005; **352**: 987–996.
2. Chatterjee S, Matsumura A, Schradermeier J, Gillespie GY. Human malignant glioma therapy using anti-alpha(v)beta3 integrin agents. *J Neurooncol* 2000; **46**: 135–144.

3. Tate MC, Aghi MK. Biology of angiogenesis and invasion in glioma. *Neurotherapeutics* 2009; **6**: 447–457.
4. Onishi M, Ichikawa T, Kurozumi K, Date I. Angiogenesis and invasion in glioma. *Brain Tumor Pathol* 2011; **28**: 13–24.
5. Kerbel R, Folkman J. Clinical translation of angiogenesis inhibitors. *Nat Rev Cancer* 2002; **2**: 727–739.
6. Vredenburgh JJ, Desjardins A, Herndon JE, 2nd *et al.* Phase II trial of bevacizumab and irinotecan in recurrent malignant glioma. *Clin Cancer Res* 2007; **13**: 1253–1259.
7. Vredenburgh JJ, Desjardins A, Herndon JE, 2nd *et al.* Bevacizumab plus irinotecan in recurrent glioblastoma multiforme. *J Clin Oncol* 2007; **25**: 4722–4729.
8. de Groot JF, Fuller G, Kumar AJ *et al.* Tumor invasion after treatment of glioblastoma with bevacizumab: radiographic and pathologic correlation in humans and mice. *Neuro Oncol* 2010; **12**: 233–242.
9. Reardon DA, Nabors LB, Stupp R, Mikkelsen T. Cilengitide: an integrin-targeting arginine-glycine-aspartic acid peptide with promising activity for glioblastoma multiforme. *Expert Opin Investig Drugs* 2008; **17**: 1225–1235.
10. Varner JA, Cheresh DA. Integrins and cancer. *Curr Opin Cell Biol* 1996; **8**: 724–730.
11. Friedlander M, Brooks PC, Shaffer RW, Kincaid CM, Varner JA, Cheresh DA. Definition of two angiogenic pathways by distinct alpha v integrins. *Science* 1995; **270**: 1500–1502.
12. Brooks PC, Clark RA, Cheresh DA. Requirement of vascular integrin alpha v beta 3 for angiogenesis. *Science* 1994; **264**: 569–571.
13. Brooks PC, Montgomery AM, Rosenfeld M *et al.* Integrin alpha v beta 3 antagonists promote tumor regression by inducing apoptosis of angiogenic blood vessels. *Cell* 1994; **79**: 1157–1164.
14. Hodivala-Dilke KM, Reynolds AR, Reynolds LE. Integrins in angiogenesis: multitalented molecules in a balancing act. *Cell Tissue Res* 2003; **314**: 131–144.
15. Leavesley DI, Ferguson GD, Wayner EA, Cheresh DA. Requirement of the integrin beta 3 subunit for carcinoma cell spreading or migration on vitronectin and fibrinogen. *J Cell Biol* 1992; **117**: 1101–1107.
16. MacDonald TJ, Taga T, Shimada H *et al.* Preferential susceptibility of brain tumors to the antiangiogenic effects of an alpha(v) integrin antagonist. *Neurosurgery* 2001; **48**: 151–157.
17. Oliveira-Ferrer L, Hauschild J, Fiedler W *et al.* Cilengitide induces cellular detachment and apoptosis in endothelial and glioma cells mediated by inhibition of FAK/src/AKT pathway. *J Exp Clin Cancer Res* 2008; **27**: 86–99.
18. Alghisi GC, Ponsonnet L, Ruegg C. The integrin antagonist cilengitide activates alphaVbeta3, disrupts VE-cadherin localization at cell junctions and enhances permeability in endothelial cells. *PLoS ONE* 2009; **4**: e4449.
19. Tucker GC. Alpha v integrin inhibitors and cancer therapy. *Curr Opin Investig Drugs* 2003; **4**: 722–731.
20. Inoue S, Ichikawa T, Kurozumi K *et al.* Novel animal glioma models that separately exhibit two different invasive and angiogenic phenotypes of human glioblastomas. *World Neurosurg* 2011. doi: 10.1016/j.wneu.2011.09.005.
21. Hampl JA, Camp SM, Mydlarz WK *et al.* Potentiated gene delivery to tumors using herpes simplex virus/Epstein-Barr virus/RV tribrid amplicon vectors. *Hum Gene Ther* 2003; **14**: 611–626.
22. Bishop ET, Bell GT, Bloor S, Broom IJ, Hendry NF, Wheatley DN. An in vitro model of angiogenesis: basic features. *Angiogenesis* 1999; **3**: 335–344.
23. Igarashi T, Miyake K, Kato K *et al.* Lentivirus-mediated expression of angiostatin efficiently inhibits neovascularization in a murine proliferative retinopathy model. *Gene Ther* 2003; **10**: 219–226.
24. Bouchard V, Demers MJ, Thibodeau S *et al.* Fak/Src signaling in human intestinal epithelial cell survival and anoikis: differentiation state-specific uncoupling with the PI3-K/Akt-1 and MEK/Erk pathways. *J Cell Physiol* 2007; **212**: 717–728.
25. Cifarelli CP, Titus B, Yeoh HK. Cadherin-dependent adhesion of human U373MG glioblastoma cells promotes neurite outgrowth and increases migratory capacity. Laboratory investigation. *J Neurosurg* 2011; **114**: 663–669.
26. Izumoto S, Ohnishi T, Arita N, Hiraga S, Taki T, Hayakawa T. Gene expression of neural cell adhesion molecule L1 in malignant gliomas and biological significance of L1 in glioma invasion. *Cancer Res* 1996; **56**: 1440–1444.
27. Yamada S, Bu XY, Khankaldyyan V, Gonzales-Gomez I, McComb JG, Laug WE. Effect of the angiogenesis inhibitor Cilengitide (EMD 121974) on glioblastoma growth in nude mice. *Neurosurgery* 2006; **59**: 1304–1312; discussion 1312.
28. Norden AD, Young GS, Setayesh K *et al.* Bevacizumab for recurrent malignant gliomas: efficacy, toxicity, and patterns of recurrence. *Neurology* 2008; **70**: 779–787.
29. Kunkel P, Ulbricht U, Bohlen P *et al.* Inhibition of glioma angiogenesis and growth in vivo by systemic treatment with a monoclonal antibody against vascular endothelial growth factor receptor-2. *Cancer Res* 2001; **61**: 6624–6628.

30. Rubenstein JL, Kim J, Ozawa T *et al.* Anti-VEGF antibody treatment of glioblastoma prolongs survival but results in increased vascular cooption. *Neoplasia* 2000; **2**: 306–314.
31. Tuettenberg J, Friedel C, Vajkoczy P. Angiogenesis in malignant glioma – a target for antitumor therapy? *Crit Rev Oncol Hematol* 2006; **59**: 181–193.
32. Platten M, Wick W, Wild-Bode C, Aulwurm S, Dichgans J, Weller M. Transforming growth factors beta(1) (TGF-beta(1)) and TGF-beta(2) promote glioma cell migration via Up-regulation of alpha(V)beta(3) integrin expression. *Biochem Biophys Res Commun* 2000; **268**: 607–611.
33. Gilbert MR, Kuhn J, Lamborn KR *et al.* Cilengitide in patients with recurrent glioblastoma: the results of NABTC 03-02, a phase II trial with measures of treatment delivery. *J Neurooncol* 2012; **106**: 147–153.
34. Reardon DA, Fink KL, Mikkelsen T *et al.* Randomized phase II study of cilengitide, an integrin-targeting arginine-glycine-aspartic acid peptide, in recurrent glioblastoma multiforme. *J Clin Oncol* 2008; **26**: 5610–5617.
35. Burke PA, DeNardo SJ, Miers LA, Lamborn KR, Matzku S, DeNardo GL. Cilengitide targeting of alpha(v)beta(3) integrin receptor synergizes with radioimmunotherapy to increase efficacy and apoptosis in breast cancer xenografts. *Cancer Res* 2002; **62**: 4263–4272.
36. Abdollahi A, Griggs DW, Zieher H *et al.* Inhibition of alpha(v)beta3 integrin survival signaling enhances antiangiogenic and antitumor effects of radiotherapy. *Clin Cancer Res* 2005; **11**: 6270–6279.
37. Tentori L, Dorio AS, Muzi A *et al.* The integrin antagonist cilengitide increases the antitumor activity of temozolomide against malignant melanoma. *Oncol Rep* 2008; **19**: 1039–1043.
38. Mikkelsen T, Brodie C, Finniss S *et al.* Radiation sensitization of glioblastoma by cilengitide has unanticipated schedule-dependency. *Int J Cancer* 2009; **124**: 2719–2727.
39. Kurozumi K, Hardcastle J, Thakur R *et al.* Effect of tumor microenvironment modulation on the efficacy of oncolytic virus therapy. *J Natl Cancer Inst* 2007; **99**: 1768–1781.

Onishi et al. SpringerPlus 2013, 2:160
http://www.springerplus.com/content/2/1/160

SpringerPlus
a SpringerOpen Journal

RESEARCH Open Access

Gene expression profiling of the anti-glioma effect of Cilengitide

Manabu Onishi[1], Kazuhiko Kurozumi[1*], Tomotsugu Ichikawa[1], Hiroyuki Michiue[2], Kentaro Fujii[1], Joji Ishida[1], Yosuke Shimazu[1], E Antonio Chiocca[3], Balveen Kaur[4] and Isao Date[1]

Abstract

Cilengitide (EMD121974), an inhibitor of the adhesive function of integrins, demonstrated preclinical efficacy against malignant glioma. It is speculated that cilengitide can inhibit tumor growth, invasion, and angiogenesis. However, the effects of cilengitide on these processes have not been sufficiently examined. In this study, we investigated the anti-glioma effect of cilengitide using DNA microarray analysis. U87ΔEGFR cells (human malignant glioma cell line) were used for this experiment. The cells were harvested after 16 h of cilengitide treatment, and mRNA was extracted. Gene expression and pathway analyses were performed using a DNA microarray (CodeLink™ Human Whole Genome Bioarray). The expression of 265 genes was changed with cilengitide treatment. The expression of 214 genes was up-regulated by more than 4-fold and the expression of 51 genes was down-regulated by more than 4-fold compared to the controls. In pathway analysis, "apoptotic cleavage of cellular proteins" and "TNF receptor signaling pathway" were over-represented. Apoptotic-associated genes such as caspase 8 were up-regulated. Gene expression profiling revealed more detailed mechanism of the anti-glioma effect of cilengitide. Genes associated with apoptosis were over-represented following cilengitide treatment.

Keywords: Glioma, Integrin, Cilengitide, Gene expression profiling, Apoptosis

Introduction

Gliomas are the most frequent primary intracranial neoplasm in adults and are invariably fatal. The median survival of aggressively treated patients with glioblastoma is approximately 14.6 months (Stupp & Weber 2005). The resistance of gliomas to the conventional therapeutic regimen of surgery, radiotherapy, and chemotherapy has prompted many investigators to seek novel therapeutic approaches for this fatal disease (Chatterjee et al. 2000). Moreover, alterations of the epidermal growth factor receptor (*EGFR*) gene are common in some forms of cancer and the most frequent is a deletion of exons 2–7. It was previously reported that this mutant receptor, called ΔEGFR, confers enhanced tumorigenicity on glioblastoma cells through elevated proliferation and reduced apoptotic rates in vivo (Narita et al. 2002).

Integrins control the attachment of cells to the extracellular matrix (ECM) and participate in cellular defense against genotoxic assaults (Hynes 2002). Integrins are expressed in tumor cells and tumor endothelial cells (Varner & Cheresh 1996a; Varner & Cheresh 1996b; Varner et al. 1995), and they play important roles in angiogenesis and invasion in glioma (Friedlander et al. 1995; Brooks et al. 1994a; Brooks et al. 1994b). αvβ3 and αvβ5 integrins regulate cell adhesion (Hodivala-Dilke et al. 2003; Leavesley et al. 1992), and inhibitors of these integrins suppress tumor growth in certain preclinical models (MacDonald et al. 2001). Therefore, integrins have attracted attention as potential therapeutic targets in glioma.

Currently, αvβ3 and αvβ5 integrin antagonists including cilengitide (EMD121974), which is a cyclic RGD-containing peptide (Xiong et al. 2001), are in clinical trials. This drug is reportedly able to penetrate the blood brain barrier (BBB) in vivo (Nabors et al. 2007). Cilengitide induces anoikis in angiogenic blood vessels and brain tumor cells in vitro (Oliveira-Ferrer et al. 2008; Alghisi et al. 2009); however, the mechanisms

* Correspondence: kkuro@md.okayama-u.ac.jp
[1]Department of Neurological Surgery, Okayama University Graduate School of Medicine, Dentistry and Pharmaceutical Sciences, 2-5-1, Shikata-cho, Kita-ku, Okayama 700-8558, Japan
Full list of author information is available at the end of the article

underlying its cytotoxic effects are not completely understood.

There have been no microarray studies to date that examined the changes in gene expression after cilengitide treatment. U87ΔEGFR cells were previously shown to have increased tumorigenicity via elevated proliferation and reduced apoptosis compared to U87 cells, which cause a more aggressive phenotype than that of the parental cell line (Narita et al. 2002). In this study, we profiled and examined the gene expression of over 57000 genes using the most comprehensive GeneChip microarrays available (CodeLink™ Human Whole Genome Bioarray), and identified differentially expressed genes between untreated glioma cells (U87ΔEGFR) and cilengitide-treated glioma cells to reveal more detail mechanism of anti-glioma effect of cilengitide.

Materials and methods

Glioma cell line and drug

Glioma cell lines, U87ΔEGFR, were seeded in tissue culture dishes (BD Falcon, Franklin Lakes, NJ, USA) and cultured in Dulbecco's Modified Eagle's Medium (DMEM) supplemented with 10% fetal bovine serum (FBS), 100 U penicillin, and 0.1 mg/mL streptomycin. U87MG, Gli36Δ5, and U251 human glioma cells were also prepared and maintained as described previously (Kambara et al. 2005). Cilengitide was generously provided by Merck KgaA and the National Cancer Institute, National Institutes of Health.

Cell surface immunofluorescence assay

U87ΔEGFR cells were seeded on 4 Chamber Polystyrene Vessel Tissue Culture Treated Glass Slides (BD Falcon, Franklin Lakes, NJ, USA) and incubated overnight. For immunofluorescence, the cells were fixed in 4% paraformaldehyde in phosphate-buffered saline (PBS) for 15 min. After the cells were fixed, they were rinsed 3 times with PBS. Nonspecific binding was blocked by incubation in a blocking buffer containing 2% bovine serum albumin in PBS for 30 min at room temperature. The cells were incubated overnight at 4°C with a mouse anti-human integrin αvβ3 monoclonal antibody (Millipore Corporation, Billerica, MA, USA) or mouse anti-human integrin αvβ5 monoclonal antibody (Abcam, Cambridge, UK) diluted 1:100 in blocking buffer. The cells were washed 3 times in blocking buffer for 5 min before incubation with a secondary anti-mouse CY3-conjugated antibody (Jackson ImmunoResearch Laboratories, Inc., West Grove, PA, USA) diluted 1:300 in blocking buffer for 2 h at room temperature in the dark. After 3 washes in PBS, the cells were counterstained with 4′, 6-diamino-2-phenylindole (DAPI; 1:500) (Invitrogen, Carlsbad, CA, USA) (100 ng/mL) for 20 min at room temperature. The slides were washed 3 times in PBS and mounted.

Water-soluble tetrazolium-1 assay

A water-soluble tetrazolium (WST)-1 assay (Roche Diagnostics) was performed according to the manufacturer's instructions. Briefly, cells treated with saline (control cells) or Cilengitide (1.0 μM) (Cilengitide was generously provided by Merck KGaA and the National Cancer Institute, NIH) were plated in a 96-well plate at a concentration of 25,000 cells/mL. Cell survival was measured at the indicated time points by adding 10 μL of a 1:3 (v/v) diluted ready-to-use WST-1 cell proliferation reagent stock solution (Roche, Mannheim). The samples were incubated for 60–240 min and absorption was measured with an MTP-120 micro plate reader (CORONA ELECTRIC Co., Ibaragi, Japan) at 450 nm wavelength using a 620 nm reference filter. After subtraction of the background absorption, the mean value of the untreated control cells was set as 100%.

Microarray analysis

U87ΔEGFR cells treated with cilengitide (1.0 μM for 16 h) and untreated control U87ΔEGFR cells were analyzed using a CodeLink™ Human Whole Genome Bioarray (Applied Microarrays, Inc., Tempe, AZ, USA). We entrusted the microarray analyses to Filgen, Inc. (Nagoya, Japan). Briefly, for each bioarray, 10 μg of cRNA in a 25 μL total volume were added to 5 μL of 5× fragmentation buffer, which was then incubated at 94°C for 20 min. Thereafter, 10 μg of fragmented cRNA, 78 μL of hybridization buffer component A, and 130 μL of hybridization buffer component B were added, and the final volume was brought up to 260 μL with water. The resultant hybridization reaction mixture was incubated at 90°C for 5 min, after which 250 μL were slowly injected into the input port of each array, and the ports were sealed with sealing strips. The bioarrays were then incubated for 18 h at 37°C while shaking at 300 rpm. A consistent hybridization time was maintained for comparative experiments. Following the incubation, the bioarrays were washed with 0.75 TNT buffer (0.10 M Tris–HCl, pH 7.6, 0.15 M NaCl, 0.05% Tween 20) and incubated at 46°C for 1 h. Each slot of the small reagent reservoir was then filled with 3.4 mL of Cy5-Streptavidin working solution, and the array was incubated at 25°C for another 30 min. Thereafter, the bioarrays were washed 4 times for 5 min each with 1 × TNT buffer at 25°C, rinsed twice in 0.1× SSC (Ambion, Austin, TX, USA)/0.05% Tween 20 for 30 s each, and immediately dried by centrifugation for 3 min at 25°C. Finally, the arrays were scanned using a GenePix4000B Array Scanner (Molecular Devices, Sunnyvale, CA, USA). A gene was defined as being upregulated when the cilengitide treatment/control average intensity ratio was >4.0, and downregulated when the cilengitide treatment/control ratio was <0.25. We performed pathway analysis on the genes that expressed increase and decrease using

Microarray Data Analysis Tool Ver3.2 (Filgen, Inc). The data were extracted using the following criteria: Z-score > 0 and P-value < 0.05 (Ichii et al. 2011; Yoshino et al. 2011).

Quantitative reverse-transcription polymerase chain reaction (QRT-PCR)

Total RNA was isolated from cultured U87ΔEGFR cells treated with cilengitide (1.0 μM for 16 h) and untreated control U87ΔEGFR cells using an RNeasy® Mini Kit (QIAGEN, Hilden, Germany). In vivo, that RNA was extracted from the brain tumor tissue of rat that had been treated with PBS or with Cilengitide with the use of TRIZOL reagent (Invitrogen, Carlsbad, CA, USA), according to the manufacturer's instructions. Those RNA were reverse transcribed with oligo dT primers using the SuperScript III First-Strand Synthesis System for RT-PCR (Invitrogen, Carlsbad, CA, USA) according to manufacturer's instructions. Primers specific for each gene were designed using Primer 3 Plus Software (http://www.bioinformatics.nl/cgi-bin/primer3plus/primer3plus.cgi) and synthesized by Invitrogen. The resulting cDNA was amplified by PCR using gene-specific primers and the 7300 Real Time PCR system (Applied Biosystems, Foster City, CA, USA) and QuantiTectTM SYBR® Green PCR Kit (QIAGEN, Hilden, Germany). A log-linear relationship between the amplification curve and quantity of cDNA in the range of 1–1000 copies was observed. The cycle number at the threshold was used as the threshold cycle (Ct). The different expression of mRNA was detected from 2-ΔΔCt using the 7300 Real Time PCR System with Sequence Detection Software (version 1.4; Applied Biosystems, Foster City, CA, USA). The amount of cDNA in each sample was normalized to the crossing point of the housekeeping gene glyceraldehyde 3-phosphate dehydrogenase (GAPDH). The following thermal cycling parameters were used: denaturation at 95°C for 10 min followed by 45 cycles at 94°C for 15 s, 50°C for 30 s, and 72°C for 30 s. The relative mRNA upregulation for each gene in the control was calculated using their respective crossing points with the following formula, as previously described (Kurozumi et al. 2007):

$F = 2^{(TH - TG) - (OH - OG)}$ where, F = fold difference, T = control, O = treated cell or tumor, H = housekeeping (GAPDH), and G = gene of interest.

CASPASE 8 primers
CASP8 F (forward), 5-TGCAGGGTCTCACTCTGTTG-3
CASP8 R (reverse), 5-TTGATTTTGGAGGGATCTCG-3
protein kinase C, zeta primers
PKCZ F (forward), 5-GTTATCGATGGGATGGATGG-3
PKCZ R (reverse), 5-GCACCAGCTCTTTCTTCACC-3
GAPDH primers
GAPDH F (forward), 5- GAGTCAACGGATTTGGTCGT-3
GAPDH R (reverse), 5-TTGATTTTGGAGGGATCTCG-3

Activity assay of caspase-3/7 and -8

Caspase-3/7 and -8 activity levels were measured using CellEvent™ Caspase-3/7 Green Detection Reagent (Invitrogen, Carlsbad, CA, USA) and the colorimetric protease assay kit (MBL, CA, USA), respectively, according to the protocol recommended by the manufacturer. Briefly, cells (5,000 cells per well) were plated in 96-well plates in triplicate and treated with cilengitide. Cilengitide (1.0 μM) was added to the medium after 24 h of incubation. The caspase solution was added at 16 h after adding cilengitide. After incubation with these substrates, the absorbance of each well was measured using a microplate reader.

TdT-mediated dUTP nick end labeling (TUNEL) assay

U87ΔEGFR cells were seeded in 6-well plates (1.0×10^4 cells/well) and cultured in DMEM supplemented with 10% FBS. Cilengitide (10 μM) was added to the medium after 24 h of incubation. After incubation for 16 h at 37°C, the cells were examined for morphological changes. Apoptotic cells were detected with the In Situ Cell Death Detection Kit (Roche, Basel, Switzerland) according to the manufacturer's instructions.

Immunoblot analysis

Using immunoblot analysis, we examined whether treatment with cilengitide induced caspase activation via caspase 8 and caspase 3. Western blotting was carried out at a high stringency, essentially as described previously (Kurozumi et al. 2004; Michiue et al. 2005a; Michiue et al. 2005b). The harvested cells with treated each concentration of drug (0.1, 1.0, 10 μM: 16 hr) or each time course (8, 16, 24 hr: 1 μM) were lysed by a sonicator in a boiled buffer containing 1% SDS. The cell lysate (50 μg) was subjected to SDS-PAGE and transferred to nitrocellulose membranes (Hybond ECL, GE Healthcare UK Ltd, England). The blots were probed with each primary antibody. Specific bands were visualized with an enhanced chemiluminescence detection kit (GE Healthcare UK Ltd, England). The following primary rabbit polyclonal antibodies were used: anti-human caspase 8 (1:500; ab44976, abcam, Inc., UK), anti-human caspase 3 (1:250; ab32125, abcam, Inc., UK), and β-actin (1:1000; Sigma-Aldrich, St. Louis, MO, USA).

Brain xenografts

All experimental animals were housed and handled in accordance with the guidelines of the Okayama University Animal Research Committee. Before implantation, 85–90% confluent U87ΔEGFR cells were trypsinized, rinsed with DMEM supplemented with 10% FBS, and centrifuged at $100 \times g$ for 5 min; the resulting pellet was resuspended in PBS, and the cell concentration was adjusted to 1.0×10^5 cells/μL. U87ΔEGFR cells (5 μL) were injected into athymic rats (F344/N-nu/nu; CLEA Japan,

Inc., Tokyo, Japan). The animals were anesthetized and placed in stereotactic frames (Narishige, Tokyo, Japan) with their skulls exposed. Tumor cells were injected with a Hamilton syringe (Hamilton, Reno, NV, USA) into the right frontal lobe (4 mm lateral and 1 mm anterior to the bregma at a depth of 4 mm) and the syringe was slowly withdrawn after 5 min to prevent reflux. The skulls were then cleaned, the holes were sealed with bone wax, and the incision was sutured. Cilengitide or PBS was administered 3 times/week intraperitoneally (1 mg/500 μL PBS), starting on day 5 after tumor cell implantation. To assess the gene expression of caspase 8 with QRT-PCR, athymic rats harboring U87ΔEGFR brain tumors were sacrificed at 18 days after tumor implantation. The tumor-bearing right hemispheres of the brains were excised and processed for RNA. For measurements of tumor cell apoptosis, athymic rats were sacrificed at 18 days after tumor implantation. The brains were removed and fixed in 4% paraformaldehyde for at least 24 h.

TUNEL staining in vivo

Snap-frozen tissue samples were embedded in optimal cutting temperature solution (Sakura Finetek Inc., Torrance, CA, USA) for cryosectioning, and 16-μm cryostat sections were cut. Apoptotic tumor cells were detected using the In Situ Cell Death Detection Kit (Roche, Basel, Switzerland) according to the manufacturer's instructions.

Statistical analysis

Student's *t* test was used to test for statistical significance. Data are presented as the mean ± standard error. All statistical analyses were performed with the use of SPSS statistical software (version 14.0; SPSS, Inc., Chicago, IL, USA).

Results

Immunohistochemical analysis of αvβ3 and αvβ5 integrins expression in U87ΔEGFR cells

Immunofluorescence assays were conducted to determine the expression of αvβ3 and αvβ5 integrins in U87ΔEGFR cells. Cultured U87ΔEGFR cells were immunopositive for αvβ3 and αvβ5 integrins (Figure 1a, b).

Cytotoxic effects of cilengitide on the U87ΔEGFR glioma cell line in vitro

The direct effects of cilengitide were investigated on glioma cells in vitro. U87ΔEGFR cells were incubated with cilengitide at concentrations of 0–10 μM; 16 h later, the cells were subjected to the WST-1 proliferation/viability assay. Cell viability after 16 h of incubation was decreased in cell cultures treated with cilengitide, reaching statistical significance at 1 μM or higher (Figure 1c). In addition, cell viability was decreased in cell cultures treated with 1 μM cilengitide, reaching statistical significance at 16 h or later (Figure 1d). These cells became sensitive to cilengitide in a concentration- and time-dependent manner.

Microarray analysis

Our cell viability assay showed that the decrease in the number of viable cells treated with 1 μM cilengitide reached statistical significance at 16 h. At that time point, differential gene expression was compared between cilengitide-treated U87ΔEGFR cells and untreated control U87ΔEGFR cells (>4 fold change, <0.25 fold change) (Figure 2a, b). There were 265 differentially expressed genes between cilengitide-treated U87ΔEGFR cells and control U87ΔEGFR cells with 214 upregulated and 51 downregulated. We further characterized the functional significance of the dysregulated genes using pathway analysis. For the upregulated genes, 20 significantly enriched pathways were identified for the differentially expressed genes between cilengitide-treated U87ΔEGFR cells and control cells (Table 1). For the downregulated genes, 7 significantly enriched pathways were identified (Table 2). Especially for the upregulated genes, the significantly enriched molecular pathways included apoptotic cleavage of cellular proteins, FasL/CD95L signaling, TNF receptor signaling pathway, and ceramide signaling pathway. Caspase 8, desmoplakin, and protein kinase C, zeta were included in these pathways and upregulated.

Validation of the microarray results

To confirm the reliability of the results from the microarray analysis, caspase 8, protein kinase C, zeta, were verified by QRT-PCR analysis (Figure 3a, b). The relative expression of caspase 8 and protein kinase C, zeta in U87ΔEGFR cells incubated with cilengitide was significantly higher than those of the cells without cilengitide by 2.25-fold and 5.78-fold, respectively ($P < 0.05$).

Capsase activation assay and caspase expression in western blotting

U87ΔEGFR cells were treated with 0.5 μM cilengitide for 16 h. Cilengitide-induced caspase-8 activity was detected with the colorimetric protease assay kit. The relative absorbance (RA) of U87ΔEGFR cell clusters were higher than control (0.27 ± 0.01 RA vs. 0.36 ± 0.01 RA, respectively; $P < 0.05$) (Figure 3a). U87ΔEGFR cells were loaded with 8 μM CellEvent™ Caspase-3/7 Green Detection Reagent then treated with the same concentration. Cilengitide-induced caspase 3/7 activity was detected with the CellEvent™ Caspase-3/7 Green Detection Reagent. The relative Fluorescence Unit (RFU) of U87ΔEGFR cell clusters were higher than control (35.4 ± 0.78 RFU vs. 16.5 ± 0.5 RFU, respectively; $P < 0.05$) (Figure 3b). The next series of experiments was designed to examine whether treatment with cilengitide induced caspase activation in other cell lines. Caspase

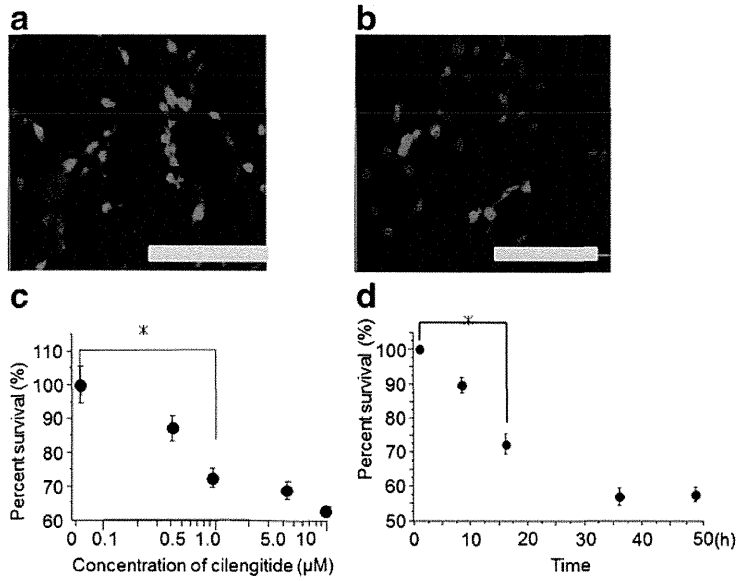

Figure 1 Immunohistochemical analysis of the αvβ3 and αvβ5 integrins, and WST-1 proliferation/viability assay. Cultured U87ΔEGFR cells were immunopositive for αvβ3 (**a**) and αvβ5 (**b**) integrins (Scale bar 100 μm). Cilengitide reduced the number of viable cells in a dose and time -dependent manner (*P < 0.05) (mean ± SE) (**c, d**).

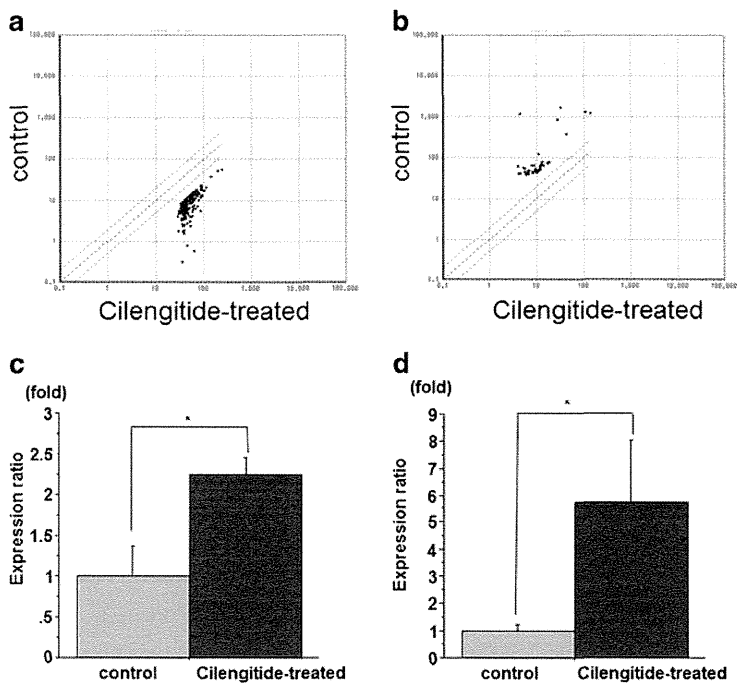

Figure 2 Microarray and QRT-PCR analyses of cilengitide-treated cells. There were 265 differentially expressed genes between cilengitide-treated U87ΔEGFR cells and untreated control U87ΔEGFR cells with 214 upregulated (**a**) and 51 downregulated (**b**) genes. Caspase-8 (**c**) and protein kinase C, zeta (**d**) were significantly increased by cilengitide treatment (*P < 0.05) (mean ± SE, n 3).

Table 1 Significantly enriched pathways between cilengitide-treated U87ΔEGFR and control

Pathwayname	Entrez gene ID	Gene symbol	P-value	Z score
NF-kB activation through FADD/RIP-1 pathway mediated by caspase-8 and -10	23586, 841	DDX58, CASP8	0.004	6.358
Organic cation/anion/zwitterion transport	55867, 6580	SLC22A11, SLC22A1	0.005	6.084
Cell adhesion molecules (CAMs)	1364, 4359, 941, :965	CLDN4, MPZ, CD80, CD58	0.014	3.213
NOSIP mediated eNOS trafficking	4846	NOS3	0.022	8.034
EPHB forward signaling	8867, 8997	SYNJ1, KALRN	0.026	3.585
Apoptotic cleavage of cellular proteins	1832, 841	DSP, CASP8	0.034	3.262
Regulation of RAC1 activity	2059, 8997	EPS8, KALRN	0.036	3.204
Activation, myristolyation of BID and translocation to mitochondria	841	CASP8	0.037	5.593
Fatty acids	1580	CYP4B1	0.037	2.177
Signaling in Immune system	23586, 3429, 6196, 6672, :841, 84433, 941	DDX58, IFI27, RPS6KA2, SP100, CASP8, CARD11, CD80	0.037	3.149
LKB1 signaling events	2011, 57521	MARK2,RPTOR	0.037	2.631
ErbB1 downstream signaling	2059, 4086, 5590	EPS8, SMAD1, PRKCZ	0.039	4.964
FasL/CD95L signaling	841	CASP8	0.044	4.964
NOSTRIN mediated eNOS trafficking	4846	NOS3	0.044	4.964
Organic anion transport	55867	SLC22A11,	0.044	4.964
Pyrimidine biosynthesis	7372	UMPS	0.044	4.964
Release of eIF4E	57521	PRTOR	0.044	4.964
Ceramide signaling pathway	5590, 841	PRKCZ, CASP8	0.046	2.899
TNF receptor signaling pathway	5590, 841	PRKCZ, CASP8	0.046	2.899
Thromboxane A2 receptor signaling	4846, 5590	NOS3, PRKCZ	0.048	2.853

activation was analyzed by using immunoblotting. Caspase 3 is produced as a 32-kDa proenzyme and cleaved into its 17 kDa active form. In U251, Gli36Δ5, U87MG, and U87ΔEGFR cells, cilengitide treatment induced the activated form of caspase 3. Caspase 8 is produced as a 55-kDa proenzyme and cleaved into its 30 kDa and 15 kDa active form. In U251, Gli36Δ5, U87MG, and U87ΔEGFR cells, cilengitide induced the activated form of caspase 9. Immunoblot analysis revealed that caspases 3 and 8 were processed in both cells in response to cilengitide in a concentration- (Figure 3c) and time-dependent manner (Figure 3d).

Apoptosis analysis

To confirm the apoptosis of the deformed glioma cells treated with cilengitide, the cells were stained with the In Situ Cell Death Detection Kit using TMR red. Originally, U87ΔEGFR cells in culture were composed of bipolar cells; however, they became spherical and agglutinated when cilengitide was added to the culture medium. Some of these deformed cells detached from the plate (Figure 4a, b, c, d). These detached U87ΔEGFR cells were not viable, as indicated by unsuccessful attempts of re-plating these cells in medium that did not contain cilengitide. U87ΔEGFR cell clusters were positive cells

Table 2 Downregulated pathway

Pathway name	Entrez gene ID	Gene symbol	P-value	Z score
Sphingolipid metabolism	8879	SGPL1	0.006	16.049
BH3-only proteins associate with and inactivate anti-apoptotic BCL-2 members	598	BCL2L1	0.015	8.496
G alpha (s) signalling events	134860, 4160	TAAR9, MC4R	0.022	3.717
Syndecan-3-mediated signaling events	4160	MC4R	0.032	5.52
Sphingosine 1-phosphate (S1P) pathway	8879	SGPL1	0.038	5.036
Signaling events mediated by the Hedgehog family	91653	BOC	0.042	4.771
Pentose phosphate pathway	8277	TKTL1	0.045	4.54